Pergamon

Tetrahedron 55 (1999) 5303–5318

TETRAHEDRON

Origin of π-Facial Stereoselection in Nucleophilic Additions of Adamantanones. A New Interpretation Based on the Exterior Frontier Orbital Extension Model

Shuji Tomoda* and Takatoshi Senju

Department of Life Sciences, Graduate School of Arts and Sciences

The University of Tokyo, Komaba, Meguro, Tokyo 153-8902, Japan

Received 4 February 1999; accepted 3 March 1999

Abstract: The experimental data of π-facial stereoselection of 5-substituted adamantan-2-ones, 5-aza-adamantan-2-ones, and nor- and homo-adamantanones have been successfully rationalized by the exterior frontier orbital extension model (EFOE model). The values of π-plane-divided accessible space (PDAS), which represents simple summation of the π-plane-divided exterior three-dimensional space nearest to the reaction center outside the van der Waals surface, showed that the adamantanone system is sterically biased and sterically much more demanding than cyclohexanone. The PDAS values indicated that in most cases steric effects are responsible for π-facial stereoselection except for a series of 5-aryladamantan-2-ones, the facial stereoselection of which was found to be orbital-controlled. In most cases, the facial differences in the frontier orbital (LUMO) extension as quantified by the EFOE density were marginal, but were consistent with experimental stereoselectivity except for a few cases with electron-withdrawing substituents. The structures of the transition states of a few 5-substituted adamantan-2-ones with $LiAlH_4$ (B3LYP/6-31+G(d)) have shown that (1) hyperconjugative *anti*-periplanar stabilization effects involving an incipient bond (AP effects) are much larger in adamantan-2-one than in cyclohexanone, in spite of enhanced reactivity with hydride of the latter, (2) the facial differences of AP effects are marginal and (3) they often operate against observed stereoselectivity.

INTRODUCTION

The origin of diastereoselection of addition reactions to unsaturated organic substrates continues to attract lively discussion.[1] Since Cieplak's proposal of his conceptual model in 1981,[2] most discussions are focused on the importance of transition state stabilization arising from the *anti*-periplanar hyperconjugative stabilization effect involving the incipient bond (hereafter abbreviated as "the AP effect") and/or from the torsional strain of substrate.[3,4] The resolution between the two opposite mechanisms of the AP effect known as the Felkin-Anh model[4] and the Cieplak model[2] has been the subject of intense investigation for these two decades (Figure 1). While the former model assumed an electron-rich transition state,[4] the latter postulated an electron-deficient incipient bond in common organic reactions.[2] As a consequence, most arguments are based on the transition state theory,[5] the theoretical basis of which has been questioned recently.[6] Nevertheless the transition state effects have rarely been evaluated quantitatively.

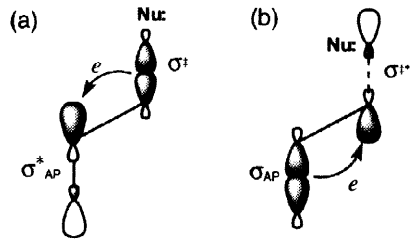

Figure 1. Mechanisms of the *anti*-periplanar hyperconjugation effect in conventional transition state models. (a); Felkin-Anh model.[4] (b); Cieplak model.[2] (**Nu**: = nucleophile)

PII: S0040-4020(99)00218-5

Recently we reported a quantitative analysis of the first transition states of carbonyl reduction with $LiAlH_4$ (LAH) using the natural bond orbital analysis[7] and proposed that the transition state effects, such as torsional strain and the AP effect, are not essential for facial diastereoselection of nucleophilic additions to some cyclic ketones including cyclohexanones and adamantan-2-ones (**1**, **2**).[8] Although it was found that the incipient bond is electron-deficient, showing the predominance of the Cieplak effect over the Felkin-Anh effect, surprisingly they often operate against observed facial stereoselectivity in adamantan-2-ones.[8]

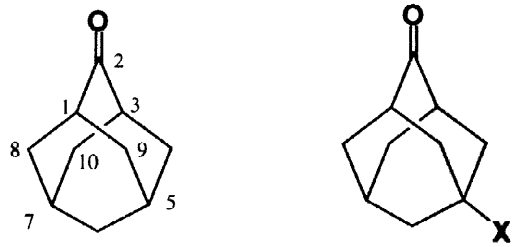

1 **2**

In the present paper, we describe full account of our theoretical approach toward understanding the essential features of π-facial stereoselection based on the exterior frontier orbital extension model (the EFOE model)[9,10] using the adamantan-2-one system for which extensive experimental data are available.

RESULTS AND DISCUSSION

Transition State Analysis

Figure 2 shows the transition state (TS) structure of LAH reduction of adamantan-2-one (**1**) optimized at the B3LYP/6-31+G(d) level.[11] Table 1 shows a comparison with cyclohexanone. The imaginary frequency of **1** (ν_i = −389.4 cm^{-1}) is very similar to those of the corresponding transition states of cyclohexanone (ν_i = −377.7 cm^{-1} and −392.6 cm^{-1} for *ax*- and *eq*-TS, respectively).[8] So is the overall structure around the reaction center. For example, comparison between the transition structure data of **1** and cyclohexanone reveals that (1) the torsion angles between the incipient bond and the vicinal *anti*-periplanar bond (the AP bond) (ϕ) are nearly the same and (2) the bond distances of $C_{=O}$–C_α are almost identical. However the length of the AP bond for **1** (C_α–C_β; 1.557 Å) is slightly longer than those of cyclohexanone (1.547 Å for *eq*-TS). The incipient bond of **1** is considerably longer (1.604 Å) than those of *eq*-TS of cyclohexanone (1.556 Å). These unique structural features suggest somewhat *earlier* transition state with slightly *larger* AP effect in **1**.

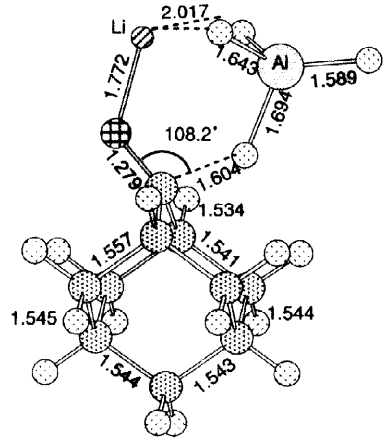

Figure 2. Transition state structure of $LiAlH_4$ reduction of adamantan-2-one (B3LYP/6-31+G(d). Bond lengths are in Å and angles are in degree.

Table 1. Selected Structural Parameters for the Transition States of Adamantan-2-one (**1**) and Cyclohexanone Reduction with $LiAlH_4$ (B3LYP/6-31+G(d))[a]

Compounds	TS	ν_i[b]	θ[c]	$C_{=O}\cdots H$[d]	ϕ[e]	H–Al	O··Li	C=O	$C_{=O}$–C_α	C_α–C_β
1	–	–389.4	108.2	1.604	168.5	1.694	1.772	1.279	1.534	1.557 1.541
cyclohexanone	*ax*	–377.7	109.8	1.531	177.6	1.709	1.764	1.284	1.531	1.536
	eq	–392.6	109.5	1.556	161.6	1.702	1.771	1.283	1.530	1.547

[a] Angles in degree and bond distances in Å. [b] Imaginary vibrational frequency (cm^{-1}). [c] The angle between the incipient bond and the carbonyl bond. [d] Distance of the incipient bond. [e] The torsion angle between incipient bond and the vicinal *anti*-periplanar bond.

It has long been known that adamantan-2-one (**1**) is less reactive with hydride than cyclohexanone. For instance, the rate constant of the reduction of **1** with $NaBH_4$ in water-dioxane mixture is 5.14 $l\cdot mole\cdot min^{-1}$, which is very close to the average value of the axial and equatorial rate constants of cyclohexanone reduction under identical conditions (8.55 and 2.15 $l\cdot mole\cdot min^{-1}$ for *ax*- and *eq*-attack, respectively).[12] On the other hand, the LAH transition state of **1** (Figure 2 and Table 1) shows more than twice (+0.34 % elongation of the C–C bond) as large AP effects as those of cyclohexanone (+0.05 % and +0.14 % for *ax*- and *eq*-TS, respectively[8]). Since the enhancement of the AP effect should lead to reduction in the energy level of transition state, factor(s) other than the AP effect must be responsible for the rate retardation[12] of hydride reduction of **1** compared with cyclohexanone.

Theoretical evidence against the positive role of the AP effect on π-facial selection may be seen in the transition state structures of 5-substituted adamantan-2-ones (**2**) whose stereochemistries of hydride reduction and MeLi reactions have been determined by elaborate experiments.[13] Table 2 collects the calculated thermochemical data of the LAH reduction transition states of two 5-substituted adamantan-2-ones (substituent = Me (**2**-Me), F (**2**-F)) and 5-azaadamantan-2-one-N-oxide (**3**) obtained at the B3LYP/6-31+G(d) level. These data are in good agreement with observed *syn* stereoselectivity. Table 3 shows the quantitative data of the AP effects at the transition states of these compounds.

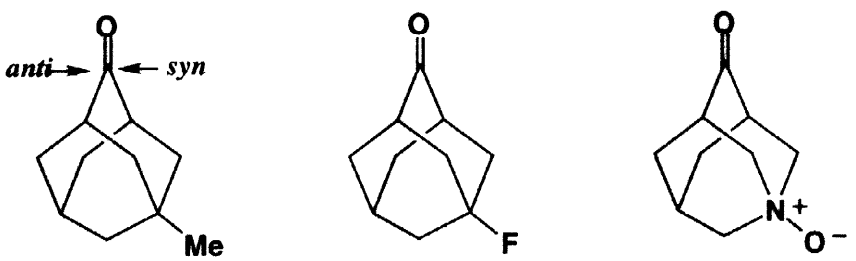

2-Me **2-F** **3**

The LAH transition states of **2**-Me show only marginal difference in % elongation[14] due to the AP effect between the *syn*- (+0.40 %) and *anti*-TS (+0.38 %) relative to the ground-state **2**-Me.[15] However, **2**-F, which gives preferential *syn*-attack in $NaBH_4$ reduction (62 : 38),[13a] shows larger AP effect in *anti*-TS (+0.48 %) than in *syn*-TS (+0.39 %) relative to ground-state **2**-F. In both of these cases, the *syn*-TS is more stable than the *anti*-TS by 0.08 (**2**-Me) and 0.09 (**2**-F) kcal mol^{-1}. Another case which shows similar behavior is 5-azaadamantan-2-one-N-oxide (**3**) which prefers 96% *syn*-attack upon reduction with $NaBH_4$.[13g] The LAH reduction transition states of **3** (Figure 3 and Table 3) show elongation of the vicinal *anti*-periplanar bonds of +1.00 % (*anti*-TS) and +0.95 % (*syn*-TS) relative to ground-state **3**. Virtually no

difference in the magnitude of the AP effects over two carbonyl faces of **3** is evident. The bond electron populations (BP) calculated with natural bond orbital analysis (NBO)[7] are in complete agreement with the magnitudes of these bond elongation data (Table 3). It is seen that in all these seven cases listed in Table 3, approximately 0.01 electrons are removed from one vicinal *anti*-periplanar bond due to the AP effect. It should be noted here that the magnitude of the AP effect seems proportional to the length of the incipient bond. Namely the longer the incipient bond, the larger the AP effect. This is consistent with the earlier observation that in general the magnitude of the AP effect steadily decreases along the way to the transition state owing to the energy rise of the incipient $\sigma_{C\cdots H}$ bond and to the elongation of the intervening σ_{CC} bond in *anti*-periplanar hyperconjugation toward transition state.[8]

Table 2. Energy Parameters for the Transition states (TS) of Adamantan-2-ones with $LiAlH_4$.[a]

Adamantanones	TS	ν_i[b]	ZPVE[c]	E[d]	$\Delta\Delta H^{\ddagger}$[e]	$\Delta\Delta G^{\ddagger}$[f]
1	–	–389.4	159.89	–717.137095	–	–
2-Me	*anti*	–391.0	177.21	–756.454486	–0.17	–0.08
	syn	–382.2	177.14	–756.454670		
2-F	*anti*	–377.2	154.76	–816.387472	–0.25	–0.09
	syn	–379.7	154.76	–816.387838		
3	*anti*	–347.7	155.50	–808.316178	–0.20	0.06
	syn	–359.2	155.58	–808.316566		

[a] B3LYP/6-31+G(d). [b] Imaginary vibrational frequency in cm^{-1}. [c] Zero point vibrational energy in kcal mol^{-1}. [d] Total electronic energy in au. [e] $\Delta\Delta H^{\ddagger} = H^{\ddagger}_{syn} - H^{\ddagger}_{anti}$ (kcal mol^{-1}). [f] $\Delta\Delta G^{\ddagger} = G^{\ddagger}_{syn} - G^{\ddagger}_{anti}$ (kcal mol^{-1}).

Table 3. The transition State Structures and the *anti*-Periplanar Effects for $LiAlH_4$ Reduction of 5-Methyladamantan-2-one (**2**-Me), 5-Fluoroadamantan-2-one (**2**-F) and 5-Azaadamantan-2-one-N-oxide (**3**) Calculated at the B3LYP/6-31+G(d) level.

Adaman-tanones	TS	θ[a]	ϕ[b]	C···H[c]	C=O	C1–C9 (%)[d]	C1–C8 (%)[d]	BP[e] C1–C9	BP[e] C1–C8
1		108.2	168.5	1.604	1.279	1.541 (–0.67%)	1.557 (+0.34%)	1.9753 (+0.0112)	1.9531 (–0.0110)
2-Me	*anti*	108.1	165.5	1.606	1.278	1.556 (+0.38%)	1.540 (–0.64%)	1.9533 (–0.0109)	1.9750 (+0.0112)
	syn	108.2	168.3	1.604	1.279	1.540 (–0.66%)	1.556 (+0.40%)	1.9752 (+0.0110)	19529 (–0.0109)
2-F	*anti*	107.6	168.1	1.665	1.271	1.558 (+0.48%)	1.541 (–0.67%)	1.9470 (–0.0120)	1.9753 (+0.0113)
	syn	107.8	168.1	1.657	1.273	1.542 (–0.59%)	1.558 (+0.39%)	1.9684 (+0.0093)	1.9528 (–0.0112)
3	*anti*	106.9	167.0	1.736	1.264	1.551 (+1.00%)	1.540 (–0.16%)	1.9539 (–0.0131)	1.9741 (+0.0111)
	syn	107.3	168.4	1.719	1.266	1.5343 (–0.06%)	1.557 (+0.95%)	1.9761 (+0.0092)	1.9516 (–0.0114)

[a] The angle of hydride approach with respect to the C=O bond. [b] Dihedral angle between the incipient bond and the vicinal *anti*-periplanar bond. [c] Distance of the incipient bond. [d] % Elongation (+) or shrinkage (–) relative to the corresponding bond distance of ground-state adamantan-2-one optimized at the B3LYP/6-31+G(d) level. Underlined numbers indicate those for the *anti*-periplanar bonds. [e] Bond population (BP) obtained with NBO[7] at B3LYP/6-31+G(d). Values in parenthesis are BP relative to that of the corresponding ground-state adamantan-2-one derivatives optimized at B3LYP/6-31+G(d).

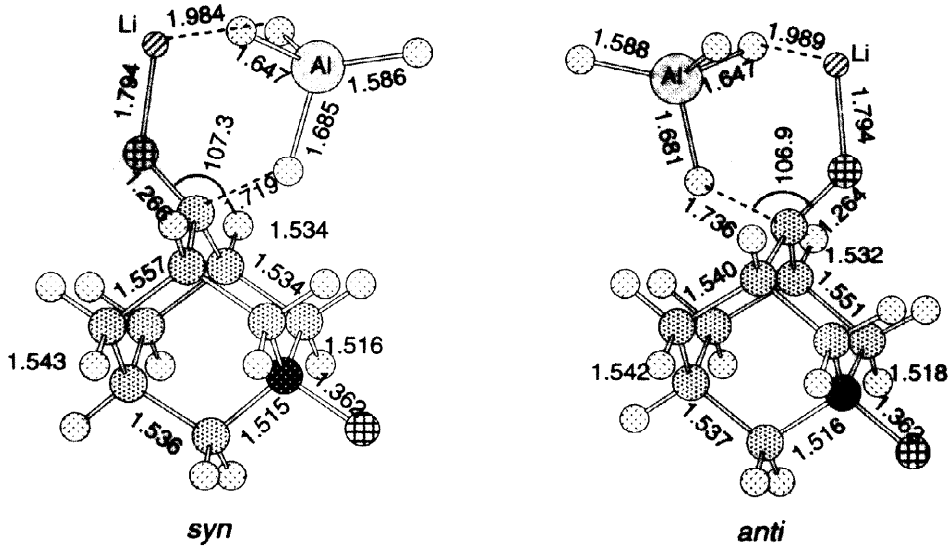

Figure 3. Transition state structures of $LiALH_4$ reduction of 5-azaadamantan-2-one-N-oxide (**3**) (B3LYP/6-31+G(d)). Bond lengths are in Å and angles are in degree.

Theoretical Description of the EFOE Model

The conclusion drawn from the above theoretical calculations of transition states is important. Namely the transition state events that have been intensively discussed for nearly two decades do not seem essential to π-facial stereoselectivity. The simplest answer to the origin of π-facial stereoselectivity would be the π-facial difference in rate constants. The Salem-Klopman equation (Eq.1)[16], a simple kinetic equation, which expresses the driving force of a chemical reaction by the summation of three independent terms, was thought to provide a reasonable basis to construct a new theory of π-facial selection.

$$\Delta E = \underbrace{-\sum_{ab}(q_a+q_b)\beta_{ab}S_{ab}}_{\text{1st term}} + \underbrace{\sum_{k<l}\frac{Q_kQ_l}{r_{kl}}}_{\text{2nd term}} + \underbrace{\sum_{r}^{\text{occ.}}\sum_{s}^{\text{unocc.}} - \sum_{s}^{\text{occ.}}\sum_{r}^{\text{unocc.}}\frac{2(\sum_{ab} c_{ra}c_{sb}\beta_{ab})^2}{E_r - E_s}}_{\text{3rd term}} \quad (1)$$

q_a, q_b = electron populations in atomic orbital a or b.
β = resonance integral, S = overlap integral
Q_k, Q_l = total electron densities at atom k or l.
r_{kl} = distance between atoms k and l.
E_r = energy level of MO r.
c = molecular orbital coefficients

The first term of Eq. 1 is the exchange repulsion term, which corresponds to the interactions among filled orbitals of the reactants. This term always leads to the destabilization of the system and is generally considered as steric effect in organic chemistry. The second term is the electrostatic interaction term that is especially important in ionic reactions. The third term is the donor-acceptor orbital interaction term, which should always lead to stabilization of the reacting system, and to which the frontier orbital interaction between reactants generally contributes most. Among these three terms, Salem and Klopman pointed out that the first and the third terms should be particularly important in common organic reactions.

The EFOE model also focuses on the first and the third terms of this equation. It is designed for quantitative evaluation of these two terms to identify essential factors of π-facial stereoselectivity of addition reactions of π-systems in general including ketones, alkenes, and enolates etc. and eventually to predict π-

facial stereoselectivity with some simple calculations and rules. Two new quantitaties – π-plane-divided accessible space (PDAS) as the steric effect term and the exterior frontier orbital extension density (EFOE density) as the orbital interaction term– constitute the new model. Both quantities focus on the exterior area of a molecule.

1. π-Plane-Divided Accessible Space (PDAS)

Steric effect is commonly introduced only as a qualitative term in organic chemistry. Highly practical asymmetric syntheses have been designed through intuitive estimation of steric effects based on the size of substituents, such as A-values[17,18] or the van der Waals radius.[19] It is however often difficult to predict steric effects of π-facial selection intuitively, in particular, for substrates having complex substituents around π-bond. A simple quantitaty of π-facial steric effect should provide convenient means to gain clearer and more effective perception in designing organic synthesis. Described herein is the first method of π-facial steric effect calculation that is useful for common organic unsaturated substrates.

The new method focuses on three-dimensional space outside the van der Waals surface of a reactant molecule.[10,20] It is based on the simple assumption that the volume of the outer (exterior) space nearest to a reaction center should contain steric information of the reactant (substrate), since this volume is precisely the three-dimensional space available for a reagent to access the reaction center of the substrate. The exterior volume is calculated for two faces of π-plane separately. Figure 4 illustrates the definition of π-plane-divided accessible space (PDAS) as a reasonable quantitative measure of π-facial steric effect using formaldehyde as an example. Molecular surface is defined as an assembly of spherical atoms having the van der Waals radii.[19] Integration of exterior three-dimensional space for the PDAS of the carbonyl carbon is performed according to the following conditions. If a three-dimensional point P(x, y, z) outside the repulsive surface is the nearest to the surface of the carbonyl carbon (a reaction center on xz plane) (*i.e.* if the distance between P and the van der Waals surface of the carbonyl carbon (d_C) is the shortest compared with the distances from P to other atomic surface (two d_H and one d_O)) and if the point is located above the carbonyl plane ($y > 0$), the space at this point is assigned to the above-space of the carbonyl carbon. The integration (summation) of such points is defined as the PDAS of the carbonyl carbon for the above-plane. For the sake of convenience, spatial integration is limited to 5 au (2.65 Å) from molecular surface, where extension of an electronic wave function is negligible beyond this limit. In general, the carbonyl plane is defined as the plane which includes the two sp^2 atoms of the π-bond and which is parallel with the vector connecting the two atoms at the α-positions. The basic concept of PDAS definition is readily extended to other π-facial steric effect in compounds containing a general double bond other than carbonyl.

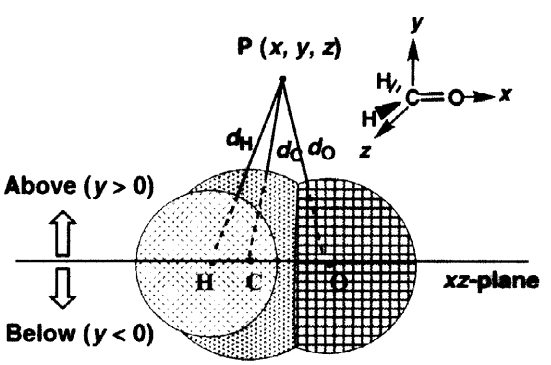

Figure 4. Definition of π-plane-divided accessible space (PDAS) for the case of formaldehyde.

The detailed calculation procedure is described in a later section. The PDAS values of cyclohexanone

are 19.4 and 47.2 au^3 for the *ax*- and the *eq*-face, respectively, suggesting that the *ax*-face is much more sterically hindered than the *eq*-face.

2. Exterior Frontier Orbital Extension Density (EFOE Density)

The importance of the exterior area of a substrate in π-facial stereoselection has also been quantified by the definition of exterior frontier orbital extension density (EFOE density), which represents the third term of Eq. 1.[16] Thus the π-plane-divided EFOE density (hereafter called simply "EFOE density") is defined as the integrated (summed) electron density of a frontier orbital (FMO; the highest occupied molecular orbital; HOMO for electrophilic addition or the lowest unoccupied molecular orbital; LUMO for nucleophilic addition)[21] over specific exterior points over one face of the π-plane of a substrate molecule satisfying the following condition: *the absolute total value of the wave functions belonging to the carbonyl carbon makes a maximum contribution to the total value of FMO wave function at the point.* Such a condition guarantees that the driving force vector on hydride or other reagent is maximally directed toward the sp^2 reaction center. Thus integration of FMO probability density (Ψ^2_{FMO}) over such three-dimensional subspace (Ω) that satisfies the above condition should afford a reasonable quantitative measure of the third term of Eq. 1. The values of EFOE density are expressed in % for the sake of numerical convenience by normalizing the wave function (Ψ_{FMO}) to 100 (Eq. 2).

$$\text{EFOE density (\%)} = 100 \times \int \Psi^2_{FMO}\, d\Omega \qquad (2)$$

Based on the Salem and Klopman equation (Eq. 1)[16] and the second-order perturbation theory[22] at the extended Hückel level,[23] a simple linear correlation between the EFOE density and activation enthalpy ($\Delta H^{\ddagger}$) can be derived assuming that EFOE density should be proportional to the overlap integral (S) between reactant FMO's. Since the frontier orbital interaction energy (ΔE) between hydride HOMO and ketone LUMO is proportional to the square of the overlap integral between these FMO's,[22,23] and this interaction occurs in one face of the carbonyl plane, assuming that the overlap integrals between the reagents (S_a and S_b) should be linearly dependent on the respective π-plane-divided EFOE density (EFOE(a) and EFOE(b)), one obtains the following equation, which describes the linear relation between λ (= EFOE(a)^2 – EFOE(b)^2) and $\Delta\Delta H^{\ddagger}$ (facial difference in activation enthalpy: $\Delta\Delta H^{\ddagger}$(b) – $\Delta\Delta H^{\ddagger}$(a)) (Eq. 3).

$$\Delta\Delta H^{\ddagger} = m\lambda + n \quad (m > 0\,;\, n : \text{a constant}) \qquad (3)$$

For a graphical plot of Eq. 3, natural log of observed stereoselectivity (product ratio) may be used if experimental $\Delta\Delta H^{\ddagger}$ is not available.

Indeed we have previously observed an excellent linear correlation (r^2 = 0.940) for the $NaBH_4$ reduction of ten alkyl-substituted cyclohexanones including compounds with high steric hindrance between the π-facial difference in the square of EFOE densities (λ = EFOE(ax)^2 – EFOE(eq)^2) and the difference in activation enthalpy for equatorial and axial attack ($\Delta\Delta H^{\ddagger} = \Delta H^{\ddagger}_{eq} - \Delta H^{\ddagger}_{ax}$).[10] In a later section, we will show another example of such a linear relationship for the 5-aryl-adamantan-2-one system.

In the subsequent sections, it will be shown using the adamantan-2-one system that both quantities (π-plane-divided accessible space (PDAS) and the EFOE density) give us a new perspective into the long-standing controversial problems on the origin of π-facial stereoselectivity.

Computational Methods

Spatial integration is limited to 5 au (2.65 Å) from molecular surface, where extension of an electronic

wave function is negligible beyond this limit. The carbonyl plane is defined as the plane which includes both sp^2 atoms of the π-bond (C=O) and which is parallel with the vector connecting the two carbon atoms at the α-positions (C1 and C3). Bondi's van der Waals radii[19] were employed for the definition of molecular surface. The calculation procedure usually begins with structure optimization at the HF/6-31G(d) level using Gaussian 94 followed by a single point calculation with "gfinput" and "pop=full" keywords at the same level.[11] For bromides, Huzinaga's 43321/4321/311(d) basis was used for Br[24] with 6-31G(d) basis for C and H. For compounds containing I or Sn, 3-21G* basis set was employed at restricted HF level..

The computer program was designed so that simultaneous calculation of both PDAS and EFOE density could be performed according to the three-dimensional lattice method with a unit lattice volume of 0.001 ~ 0.008 au^3 (1.48×10^{-4} ~ 1.18×10^{-3} Å^3). The quality of each EFOE calculation was checked by the value of the total electron density, which converged nearly unity (1.000 ± 0.001). All calculations were carried out on a Silicon Graphics Power Indigo II or an IBM SP2 computer.

Application of the EFOE Model

1. 5-Substituted-2-Adamantan-2-ones

Extensive experimental studies on the π-facial stereoselection of adamantan-2-ones (**2**) have been reported.[13] The high-quality data should offer a unique opportunity to test the utility of the EFOE model. The adamantan-2-one system was adopted as an ideal probe to delineate the electronic effects on π-facial stereoselection in the absence of steric effects without conformational uncertainties.[13] Both carbonyl π-faces were assumed to be sterically equivalent in the conformationally rigid and sterically unbiased carbon framework. It will be shown later that this is an effective strategy only for one case of adamantan-2-one series (5-aryladamantan-2-ones (**7**)), where facial steric difference uniquely remains unchanged within the group of compounds.[13e] We show here that in general the π-bond of the adamantanone system is sterically biased.

The 2-adamantanone derivatives employed thus far are 5-substituted adamantan-2-ones (**2**, **7**),[13a-e] 5-azaadamantan-2-ones (**3**, **4**, **5**),[13g] adamantan-2-thiones (**6**),[13i] 4,9-substituted adamantan-2-ones (**8**),[13h] perfluoroadamantan-2-ones (**9**),[13j] nor- and homoadamantan-9-ones (**10**, **11**).[13k] le Noble tentatively rationalized a large amount of his stereoselectivity data in terms of the Cieplak hyperconjugation model.[2] Central to his interpretation is the observation of a good linear Hammett type plot for the $NaBH_4$ reductions of *p*-substituted 5-phenyladamantan-2-ones.[13d] However, the importance of hyperconjugative interactions in hydride reduction of adamantanones has recently been questioned by two groups. Adcock found an excellent proportional correlation between product ratio and polar substituent effects.[13e] He suggested that direct electrostatic field interactions should play a dominant role in governing the facial stereoselection in nucleophilic carbonyl additions.[13e] Very recently, Gung concluded based on *ab initio* MO calculations as well as by re-examination of the X-ray data reported previously that the adamantanone system is often "sterically biased", which is the major origin of the facial stereoselection in nucleophilic additions of adamantanones.[25]

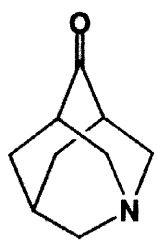

4

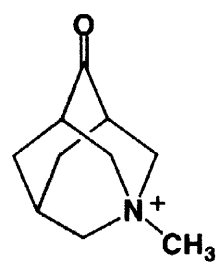

5

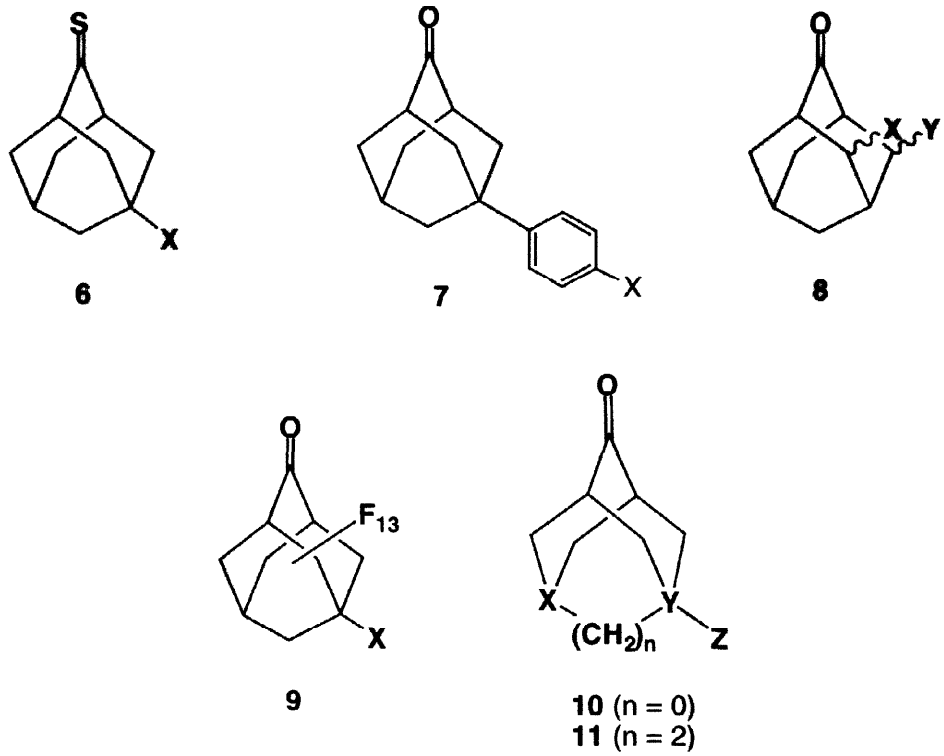

6 7 8

9

10 (n = 0)
11 (n = 2)

The EFOE analysis on the adamantanone system has revealed that the three terms of the Salem-Klopman equation (Eq. 1)[16] – the exchange repulsion term (steric effect), the electrostatic term and the donor-acceptor interaction term – are all responsible for π-facial selection. In many cases, the experimental data are consistent with the PDAS values owing to the intrinsic sterically-demanding nature of the adamantanone system as described below. The EFOE densities are consistent with most experimental facial selections. In particular, a series of 5-aryladamantan-2-ones (**7**), where facial difference in the PDAS values are nearly identical, showed a remarkable linear correlation of the EFOE plot according to Eq. 3. These results are discussed later.

Table 4 collects the results of the EFOE analyses for 5-substituted adamantan-2-ones (**2**), adamantan-2-one-5-N-oxide (**3**), 5-azaadamantan-2-one (**4**) and its methyl ammonium (**5**) and 5-substituted adamantan-2-thiones (**6**). The PDAS values of adamantan-2-one are both 11.1 au^3, which is much smaller in size than that of the *ax*-face of cyclohexanone (19.4 au^3). This implies that adamantan-2-one is much *more sterically demanding* than cyclohexanone. This in turn suggests that adamantanone may be more sensitive to a change in steric environment than cyclohexanone. Namely, subtle changes in steric environment around the carbonyl of adamantan-2-one may cause significant difference in facial stereoselection.

The EFOE value of adamantan-2-one (**1**) (1.097, 1.098) is nearly equal to the average value of those of cyclohexanone (1.940(*ax*) and 0.249 (*eq*)). This is consistent with the earlier comparison of the rate data of $NaBH_4$ reduction with that of cyclohexanone.[12] Among 31 examples of adamantan-2-ones (**2–5**) and the corresponding thiones (**6**), the values of EFOE density correctly predicts experimental stereochemistry of hydride reduction with the exception of seven subtle cases (X = *t*-Bu, Cl, NMe_2, CO_2Me, CF_3, $SiMe_3$, $SnMe_3$), whereas the PDAS values predict correctly except for five cases (X = *t*-Bu, O^-, NMe_2, NMe_3^+, CO_2^-). The behavior of the three charged substituents (X = O^-, NMe_3^+, CO_2^-) can be interpreted with the electrostatic term of Eq. 1,[16] but the stereoselection of NMe_2 (lone-pair outside conformation) is a puzzle. In the latter case, the lone-pair inside conformation could not be optimized. All the substituents have a larger

Table 4. EFOE Analysis of 5-Substituted(X) adamantan-2-ones (**2**), 5-Azaadamantan-2-ones (**3**, **4**, **5**) and 5-Substituted(X) Adamantan-2-thiones (**6**).[a]

Compd.	X	EFOE Density (%)		PDAS (au^3)		ω^b (au^3)	Obs. (%) NaBH$_4$	Obs. (%) MeLi
		anti	*syn*	*anti*	*syn*		*anti* : *syn* [c]	*anti* : *syn* [d]
	H	1.097	1.098	11.1	11.1	0.0	50 : 50	50 : 50
	Me	0.996	1.153	10.7	11.2	0.5	49 : 51	46 : 54
	^{t}Bu	1.095	1.028	11.1	10.7	–0.5	50 : 50	58 : 42
	Ph [e]	1.076	1.091	10.7	11.9	1.2	45 : 55	38 : 62
	F [f]	1.032	1.068	10.3	12.7	2.4	41 : 59	34 : 66
	Cl	1.092	0.904	10.5	12.5	2.0	38 : 62	38 : 62
	Br [g]	0.946	1.231	10.6	11.8	1.2	41 : 59	40 : 60
	I [h]	0.894	0.988	10.9	11.5	0.6	40 : 60	43 : 57
	OH	1.055	1.108	10.9	11.2	0.3	42 : 58	–
	OMe (1) [i]	1.102	1.026	10.8	10.7	–0.1	36 : 64	37 : 63
	OMe (2) [j]	1.088	1.021	10.4	11.8	1.4	36 : 64	37 : 63
	O^-	1.361	0.910	10.6	11.4	0.8	51 : 49	–
2	NH_2	0.932	1.072	10.3	11.7	1.4	34 : 66	–
	NMe_2 [i,k]	1.130	1.017	11.3	10.5	–0.8	35 : 65	37 : 63
	NMe_3^+	0.285	0.674	11.9	9.9	–2.0	14 : 86	–
	PMe_3^+	0.711	0.093	12.2	9.7	–2.5	–	–
	CN	1.006	1.176	10.6	11.7	1.1	31 : 69	32 : 68
	CO_2Me	1.102	1.076	10.4	11.6	1.2	39 : 61	45 : 55
	CO_2H	1.046	1.103	10.4	11.5	1.1	48 : 52	–
	CO_2^-	1.209	1.002	9.6	12.7	3.1	55 : 45	–
	CF_3	1.103	1.051	10.4	11.6	1.2	41 : 59	28 : 72
	NO_2	1.079	1.037	10.2	12.1	2.0	25 : 75	–
	$SiMe_3$	0.922	1.115	11.3	10.6	–0.7	51 : 49	51 : 49
	$SnMe_3$ [h]	0.740	0.909	11.8	10.5	–1.3	53 : 47	52 : 48
	CPh_3 [e]	1.151	0.850	11.5	10.7	–0.8	–	–
3	–	0.951	1.144	9.6	13.7	4.1	4 : 96	–
4	–	1.054	1.156	10.2	11.5	1.3	38 : 62	–
4-Li	–	0.773	0.999	11.9	10.7	–1.2	–	62 : 38
5	–	0.385	1.164	10.3	12.4	2.1	12 : 88	–
	F	0.307	0.344	5.9	6.8	0.9	–	31 : 69[l]
6	Cl	0.309	0.330	6.0	6.7	0.7	–	35 : 65[l]
	Br	0.309	0.325	6.0	6.5	0.5	–	39 : 61[l]

[a] Structures optimized at the HF/6-31G(d) level unless otherwise specified. Huzinaga's 43321/4321/311(d) split valence basis was used for Br.[24] [b] ω = PDAS(*syn*) – PDAS(*anti*). [c] Ref. 13. Newer data were indicated. [d] Ref. 13a and 13e. Newer data were indicated. [e] LUMO+2. [f] Structure was optimized at the B3LYP/6-31+G(d) level. [g] LUMO+1. [h] HF/3-21G*. [i] The lone-pair outside the ring. [j] The lone-pair inside the ring. This conformation is more stable than the other. [k] The lone-pair inside conformation was unstable. [l] Cycloaddition with benzonitrile oxide. Ref. 13i.

PDAS value in the *syn*-face (ω = PDAS(*syn*) – PDAS(*anti*) > 0) except for bulky substituents, such as *t*-Bu, OMe(1) (the lone-pair outside conformation), NMe_2, NMe_3^+, PMe_3^+, $SiMe_3$, $SnMe_3$, CPh_3 (ω < 0).

In all these cases, one Me or Ph is situated toward the carbonyl at C2, causing some decrease in the PDAS value in the *syn*-face. The effect of substituent size on facial stereochemistry is also seen in the halogen series for the ketones (**2**) and the thiones (**6**): ω value decreases steadily on going from F to I and simultaneously the *anti*:*syn* product ratio decreases. It is generally seen that a bulky substituent reduces the carbonyl cavity over the *syn*-face, thereby decreasing the *syn*-preference of facial stereochemistry. The high *syn* selection for the ammonium ion (**5**) (*anti* : *syn* = 12 : 88) and the 5-N oxide (**3**) (*anti* : *syn* = 4 : 96) can be explained by the large π-facial difference in the EFOE density and PDAS value without assuming the Cieplak model.[2]

It is highly likely that the electronic effect[13e] and the size of a 5-substituent may cause structural deformation of the adamantanone skeleton, which should affect the PDAS values, and ultimately the overall facial selection. Figure 5 shows a plot of the facial difference in the PDAS values (ω) between the two faces against the natural log of the product ratios (p = ln (*syn*/*anti*)) for all adamantan-2-ones indicated in Table 4. A (linear) correlation between these parameters is observed for both hydride reduction (r^2 = 0.58) and MeLi addition (r^2 = 0.78) except for a few charged substituents (NMe_4^+, CO_2^-) (Figure 5). Furthermore, all the data except for the charged substituents and NMe_2 fall in the domain ($\omega > 0$ and $p > 0$) or ($\omega < 0$ and $p < 0$). This strongly indicates that in the adamantan-2-one system, where π-facial difference in frontier orbital extension is marginal, subtle steric effect may be more important for facial stereoselection in agreement with Gung's recent analysis of 5-azaadamantan-2-one-N-oxide (**3**).[25]

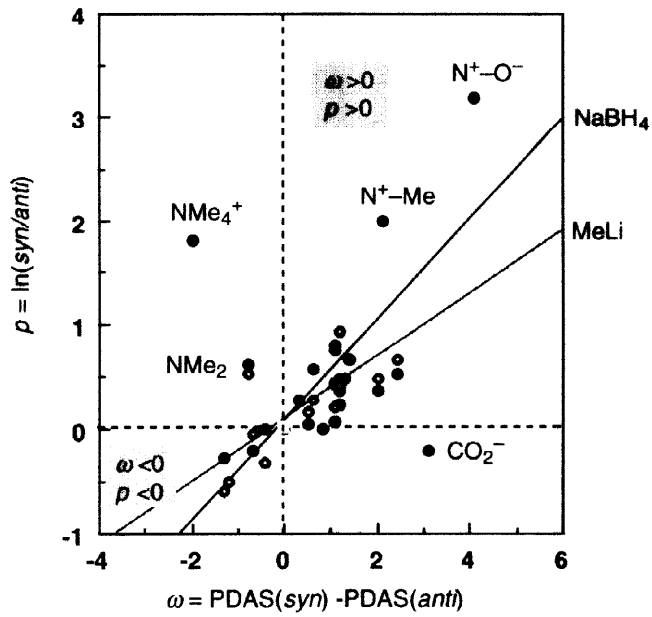

Figure 5. Correlation between the difference in PDAS values (ω = PDAS(*syn*) -PDAS(*anti*)) and product ratio (p = ln(*syn*/*anti*)) for adamantan-2-ones (Table 4). Filled circles; $NaBH_4$ reduction (r^2 = 0.58). Open circles; MeLi addition (r^2 = 0.78).

The stereochemical reversal observed for the reactions of **4** with hydride and MeLi has not been successfully explained in terms of the transition state models.[13g] However, the EFOE model correctly predicts the facial steric difference of **4**-Li, in which a Li cation coordinates at the nitrogen, is opposite (ω = −1.2 au^3) to that of parent **4** (ω = 1.3 au^3), clearly indicating that the facial steric difference is reversed by

coordination of Li cation at the nitrogen atom in the MeLi reaction. Again, it is strongly suggested that the ground-state conformational change may be responsible for the observed reversal of stereoselection.

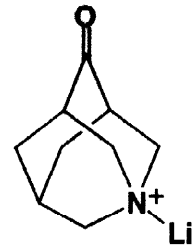

4-Li

The EFOE analysis of three 5-substituted adamantan-2-thiones (**6**)[13i] were performed. Both the EFOE density and the steric parameters are consistent with the observed stereoselectivity of cycloaddition with benzonitrile oxide without exception. In all these cases the PDAS values for the thiocarbonyl carbon are much reduced compared with those for the carbonyl of **2** due to the large sulfur atom.

2. 5-Aryl-Adamantan-2-ones

In contrast to the adamantanone derivatives shown in Table 4, when steric effect is maintained constant, subtle changes in EFOE density becomes a predominant factor of π-facial selection. The important role of the third term (the donor-acceptor interaction term) in the Salem-Klopman equation[16] can be seen in the EFOE analysis of a series of 5-(*p*-X-substituted-phenyl)adamantan-2-ones (**7**). Table 5 and Figure 6

Table 5. EFOE Density, PDAS and Observed Stereoselectivity of 5-(*p*-Substituted(X)-phenyl)adamantan-2-ones (**7**).[a]

X	EFOE Density[b] (%)		λ^c	PDAS (au^3)[b]		Obs. (%)[d] $NaBH_4$	Obs. (%)[d] MeLi
	anti	*syn*		*anti*	*syn*	*syn* : *anti*	*syn* : *anti*
NMe_2	1.0798	1.0667	–0.0281	10.63	11.29	57 : 43	57 : 43
OMe	1.0810	1.0575	–0.0503	10.72	11.25	59 : 41	59 : 41
H	1.0735	1.0602	–0.0284	10.68	11.22	58 : 42	62 : 38
F	1.0736	1.0772	0.0077	10.70	11.21	63 : 37	67 : 33
CO_2Me	1.0655	1.0815	0.0343	10.61	11.31	64 : 36	68 : 32
CN	1.0585	1.0873	0.0618	10.71	11.21	66 : 34	72 : 28
NO_2	1.0478	1.1001	0.1123	10.65	11.25	68 : 32	–

[a] HF/6-31G(d). [b] The EFOE analysis was performed with 0.001 au^3 lattice volume unsing LUMO+2 ($\pi_{C=O}^*$). [c] λ = EFOE(*syn*)^2 – EFOE(*anti*)^2. [d] Ref. 13f.

show the results of the EFOE analysis of **7**. The PDAS values shown in Table 5 guarantee that the steric effects of the system remain essentially unchanged within the series of compounds (10.6 ~ 10.7 au^3 for the *anti*-face and 11.2 ~ 11.3 au^3 for the *syn*-face), although the π-plane is sterically non-equivalent. The observed facial stereoselectivities for both reactions ($NaBH_4$ reduction and MeLi) not only show uniformly *syn*-preference for all substituents owing to the steric bias but also exhibit remarkable dependence on the EFOE densities. Figure 6 depicts the EFOE plot of the system according to Eq.3 (the natural log of product ratios are used instead of $\Delta\Delta H^{\ddagger}$). Although the changes in the values of λ (= EFOE(*syn*)^2 – EFOE(*anti*)^2) are marginal, the remarkable linear correlations for both the reduction and the methylation[13f]

unambiguously demonstrate that the facial difference in the frontier orbital extension is also an important factor in facial selection of the adamantanone system. Thus the behavior of facial selection of the 5-(*p*-X-substituted phenyl)adamantan-2-one (**7**) series can be rationalized by the EFOE model without assuming the electrostatic effect.[13e,f]

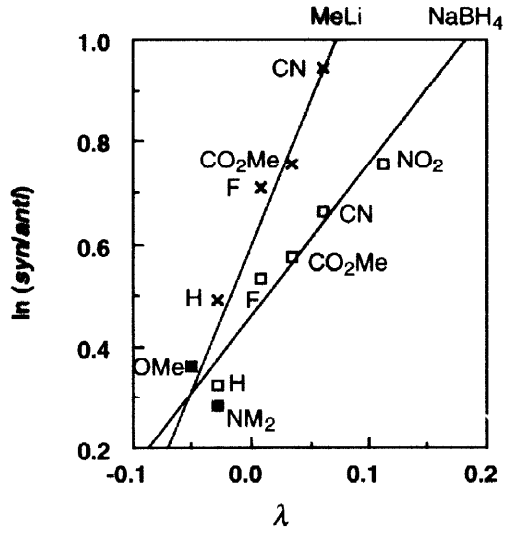

Figure 6. Plot of λ (EFOE(*syn*)^2 – EFOE(*anti*)^2) *vs.* facial selectivity (ln (*syn/anti*)) for 5-(*p*-X-substituted phenyl)adamantan-2-ones (**7**). Open squares: $NaBH_4$ in methanol (r^2 = 0.90) ; crosses: MeLi (r^2 = 0.89).

3. Other Adamantanones

The EFOE model successfully explains nucleophilic additions of other adamantanone derivatives such as 4,9-substituted adamantan-2-one (**8**),[13h] perfluoroadamantanones (**9**),[13j] and nor- and homo-9-adamantanones (**10**, **11**)[13k] as well (Tables 6, 7 and 8). In **8**, both the EFOE density and the PDAS values explain the observed stereoselectivity except for the third and the last case for which the experimental stereoselectivity has not been reported (Table 6), while in **9**, the EFOE parameters give ambiguous predictions (Table 7). In the latter cases (**9**), the PDAS values fall in the range 4.0 ~ 4.7 au^3, which is considerably sterically congested. In the case of 5-chloro-perfluoroadamantan-one (**9**-Cl), since the facial difference in the PDAS values is much larger than that of perfluoroadamantanone (**9**-H), steric effects may well be more predominant. Table 8 collects the EFOE data of nor- and homoadamantanones (**10**, **11**) recently reported along with 5-substituted adamantan-2-ones for comparison.[13k] As the length of bridging methylene (n) between atoms X and Y gets longer, the PDAS values tend to decrease due to the buttressing effect of the bridging carbons, resulting in considerable increase in steric congestion around the carbonyl. In all cases examined, the EFOE data and the positive values of ω are completely consistent with the experimental stereoselectivity. The stereochemical reversal of 3-azanoradamantanone (**10**-N) upon reaction with MeLi may also be explained by the facial difference in the EFOE density of its lithium complex (**10**-NLi).

Table 6. EFOE Analysis and Observed Stereoselectivity of 4,9-Substituted Adamantan-2-ones (**8**).[a]

X	Y	EFOE Density (%)		PDAS (au^3)		ω^b	Obs. (%)[c]	
		anti	*syn*	*anti*	*syn*	(au^3)	*anti*	*syn*
ax-F	H	1.048	0.767	9.7	8.4	–1.3	100	0
eq-F	H	1.044	1.226	10.6	11.5	0.9	33	67
eq-F	*eq*-F	0.961	1.211	10.1	12.0	1.9	–	–
ax-OH	H	0.935	0.821	10.2	7.5	–2.7	95	5
eq-OH	H	1.093	0.998	10.5	10.7	0.2	30	70[d]

[a] HF/6-31G(d). [b] ω = PDAS(*syn*) – PDAS(*anti*). [c] $NaBH_4$ in methanol. Ref.13h. [d] Calculated values form Ref. 13h

Table 7. EFOE Analysis and Observed Stereoselectivity of 5-Substituted(X) Perfluoroadamantanones (**9**).[a]

X	EFOE Density (%)		PDAS (au^3)		ω^b	Obs. (%)[c]	
	anti	*syn*	*anti*	*syn*	(au^3)	*anti*	*syn*
H	0.430	0.403	4.74	4.71	–0.03	58	42
Cl	0.379	0.385	4.34	4.08	–0.26	55	45

[a] HF/6-31G(d). [b] ω = PDAS(*syn*) – PDAS(*anti*). [c] $NaBH_4$ in methanol. Ref. 13j.

Table 8. EFOE Analysis and Product Ratio of Nor- and Homo-9-adamantanones (**10**, **11**).[a]

Compds.	n	X	Y	Z	EFOE Density (%)		PDAS (au^3)		ω^b (au^3)	Obs. (%) $NaBH_4$[c]	Obs. (%) MeLi[c]
					anti	*syn*	*anti*	*syn*		*anti* : *syn*	*anti* : *syn*
10-F	0	C	C	F	1.167	1.280	14.4	16.0	1.6	40 : 60	–
2-F	1	C	C	F	1.032	1.068	10.3	12.7	2.4	38 : 62	30 : 70
11-F	2	C	C	F	1.063	0.963	9.0	10.9	1.9	34 : 66	33 : 67
10-Br	0	C	C	Br	1.089	1.253	14.5	15.9	1.4	40 : 60	–
2-Br	1	C	C	Br	0.946	1.231	10.6	11.8	1.2	41 : 59	40 : 60
11-Br	2	C	C	Br	0.806	1.269	9.2	10.1	1.1	–	–
10-N	0	C	N	–	1.147	1.215	15.6	16.5	0.9	34 : 66	–
10-NLi	0	C	N	Li	1.073	0.888	15.3	16.2	0.9	–	55 : 45
4	1	C	N	–	1.054	1.156	10.2	11.5	1.3	38 : 62	62 : 38
11-N	2	C	N	–	0.938	1.175	9.9	10.2	1.3	–	–
10-NMe	0	C	N^+	CH_3	0.670	1.241	14.2	17.7	3.5	13 : 87	–
5	1	C	N^+	CH_3	0.385	1.164	10.3	12.4	2.1	12 : 88	–
11-NMe	2	C	N^+	CH_3	0.894	0.443	9.1	9.7	0.6	–	–
10-NO	1	N	N^+	O^-	0.951	1.144	9.6	13.7	2.9	12 : 88	–
11-NO	2	N	N^+	O^-	0.965	1.032	8.3	12.3	4.0	17 : 83	–

[a] HF/6-31G(d). Huzinaga's 43321/4321/311(d) split valence basis was used for Br.[24] [b] ω = PDAS(*syn*) – PDAS(*anti*). [c] Ref. 13k.

CONCLUSIONS

The EFOE analyses of adamantan-2-ones and the related systems have revealed that the system chosen by le Noble and Adcock turns out to be a suitable model to examine both the facial steric effect and the orbital interaction effect. It was found that (1) the facial stereoselection is most likely to be dictated chiefly by steric effect rather than the transition state *anti*-periplanar effect in 5-substituted adamantanones (Figure 5), (2) in a few cases, where charged substituents are involved, the electrostatic effect may become dominant and (3) on the other hand the substituent effect of the π-facial selection of 5-aryladamantan-2-ones (**7**) is exclusively orbital-controlled (Figure 6). Namely, the three terms of the Salem-Klopman equation (Eq.1)[16] are found to be sufficient to explain all the experimental data.[13] Thus the overall facial stereoselection of the adamantanone system can be reasonably explained by the ground-state factors including complexation with Li without invoking transition state effects.

We have demonstrated the utility of the EFOE model so far on the cyclohexanone system,[8,9] Mehta's polycyclic systems,[26] and the adamantan-2-ones and the related systems. Our preliminary calculations have indicated that the approach is applicable to the electrophilic additions of alkenes and lithium enolates as well. Full details will be reported in due course.

Acknowledgements:

We thank the Ministry of Education, Science, Sports, and Culture for financial support through Grants-in-Aid for Scientific Research (Project Nos. 09440215 and 09239207) and the Institute for Molecular Science for generous assignment of computational time.

References and Notes

(1) Gung, B. W. *Tetrahedron* **1996**, *52*, 5263.
(2) Cieplak, A. S. *J. Am. Chem. Soc.* **1981**, 103, 4540.
(3) Wu, Y. D.; Houk, K. N. *J. Am. Chem. Soc.* **1987**, *109*, 908.
(4) (a) Chérest, M.; Felkin, H. *Tetrahedron Lett.* **1968**, 2205. (b) Chérest, M.; Felkin, H.; Prudent, N. *Tetrahedron Lett.* **1968**, 2199. (c) Anh, N. T.; Eisenstein, O.; Lefour, J. -M.; Tran Huu Dau, M. E. *J. Am. Chem. Soc.* **1976**, *95*, 6146. (d) Anh, N. T.; Eisenstein, O. *Nouv. J. Chim.* **1976**, *1*, 61.
(5) Glasstone, S.; Laidler, K. J.; Eyring, H. *Theory of Rate Processes*, McGraw-Hill: New York, 1940.
(6) Carpenter, B. K. *Acc. Chem. Res.* **1992**, *25*, 520.
(7) (a) Reed, A. E.; Curtiss, L. A.; Weinhold, F. *Chem. Rev* , **1988**, 88, 899. (b) Glendening, E. D.; Weinhold, F. *Natural Resonance Theory I. General Formalism*; Technical Report of Theoretical Chemistry Institute, No. 803 (1994).
(8) Tomoda, S; Senju, T. *Chem. Commun.* **1999**, in press.
(9) Tomoda, S.; Senju T. *Tetrahedron*, **1997**, *53*, 9057.
(10) Tomoda, S; Senju, T. *Tetrahedron* **1999**, in press.
(11) Gaussian 94 (Revision D.1 and E.2); Gaussian, Inc., Pittsburgh, PA, 1997; Frisch, M. J.; Trucks, G. W.; Head-Gordon, M.; Gill, P. M. W.; Wong, M. W.; Foresman, J. B.; Johnson, B. G.; Schlegel, H. B.; Robb, M. A.; Replogle, E. S.; Gomperts, R.; Andres, J. L.; Raghavachari, K.; Binkley, J. S.; Gonzalez, C.; Martin, R. L.; Fox, D. J.; Defrees, D. J.; Baker; J.; Stewart, J. J. P.; Pople, J. A., Gaussian, Inc., Pittsburgh, PA, 1992. Gaussian 94 (Revision D.1); Frisch, M. J.; Trucks, G. W.; Schlegel, H. B.; Gill, P. M. W.; Johnson, B. G.; Robb, M. A.; Cheeseman, J. R.; Keith, T.; Petersson, G. A.; Montgomery, J. A.; Raghavachari, K.; Al-Laham, M. A.; Zakrzewski, V. G.; Ortiz, J. V.; Foresman, J. B.; Cioslowski, J.; Stefanov, B. B.; Nanayakkara, A.; Challacombe, M.; Peng, C. Y.; Ayala, P. Y.; Chen, W.; Wong, M. W.; Andres, J. L.; Replogle, E. S.; Gomperts, R.; Martin, R. L.; Fox, D. J.; Binkley, J. S.; Defrees, D. J.;

Baker, J.; Stewart, J. P.; Head-Gordon, M.; Gonzalez, C.; Pople, J. A.

(12) Geneste, P.; Lamaty, G.; Moreau, C.; Roque, J-P. *Tetrahedron Lett.* **1970**, *57*, 5011.

(13) (a) Cheung, C. K.;. Tseng, L. T; Lin, M. -H.; Srivastava, S.; le Noble, W. J. *J. Am. Chem. Soc.* **1986**,*108*, 1598. (b) Xie, M. ; le Noble, W. J. *J. Og. Chem.* **1989**, *54*, 3836. (c) le Noble, W. J.; Srivastava, S. ; Cheung, C. K. *J. Org. Chem.* **1983**, *48*, 1099. (d) Li, H.; le Noble, W. J. *Tetrahedron Lett.* **1990**, *31*, 4391. (e) Adcock, W.; Trout, N. A. *J. Org. Chem.* **1991**, *56*, 3229. (f) Adcock, W.; Cotton, J.; Trout, N. A. *J. Org. Chem.* **1994**, *59*, 1867. (g) Hahn, J. M.; le Noble, W. J. *J. Am. Chem. Soc.* **1992**, *114*, 1916. (h) Kaselj, M.; le Noble, W. J. *ibid.* **1996**, *61*, 4157. (i) Chung, W-S.; Tsai, T-L; Ho. C. C.; Chiang, M. Y. N; le Noble, W. J. *J. Org. Chem.* **1997**, *62*, 4672. (j) Kaseij, M.; Adcock, J. L; Luo, H.; Zhang, H.; Li, H.; le Noble, W. J. *J. Am. Chem. Soc.* **1995**, *117*, 7088. (k) Kaseij, M ; Gonikberg, E. M.; le Noble, W. J. *J. Org. Chem.* **1998**, *63*, 3218.

(14) % Elongation = $(\Delta r / r_s) \times 100$, where Δr = the difference in bond lengths between the vicinal *anti*-periplanar (AP) bond in transition state (r_{TS}) and the corresponding bond of starting ketone (r_s); $\Delta r = r_{TS} - r_s$. Both structures (transition state and the starting ketone) were optimized at the same level of calculation method and basis set (B3LYP/6-31+G(d)).

(15) "*Syn* and *anti*" denotes the direction of hydride attack with respect to the substituted at C5 or N5.

(16) (a) Klopman, G. *J. Am. Chem. Soc.* **1968**, *90*, 223. (b) Salem, L. *J. Am. Chem. Soc.* **1968**, *90*, 543. (c) Fleming, I. *Frontier Orbitals and Organic Chemical Reactions;* John Wiley & Sons: London, 1977.

(17) Eliel, E. L.; Wilen, S. H.; Mander, L. N. *Stereochemistry of Organic Compounds*; p.695, John Wiley & Sons: New York, 1994.

(18) Winstein S.; Holness, N. J. *J. Am. Chem. Soc.* **1955**, *89*, 5562.

(19) Bondi, A. *J. Phys. Chem.* **1964**, *68*, 441.

(20) Ohno, K.; Matsumoto, S.; Harada, Y. *J. Chem. Phys.* **1984**, *81*, 4447.

(21) (a) Fukui, K. *Theory of Orientation and Stereoselection*; Springer Verlag: Heidelberg, 1979. (b) Fukui, K.; Fujimoto, H. *Frontier Orbitals and Reaction Paths*; World Scientific: London, 1997.

(22) (a) Imamura, A. *Mol. Phys.* **1968**, *15*, 225–238. (b) Libit, L.; Hoffmann, R. *J. Am. Chem. Soc.* **1974**, *96*, 1370. (c) Inagaki, S.; Fujimoto, H.; Fukui, K. *J. Am. Chem. Soc.* **1976**, *98*, 4054.

(23) Hoffmann, R. *J. Chem. Phys.* **1963**, *39*, 1397.

(24) Huzinaga, S.; *Gaussian Basis Sets for Molecular Calculations*; Elsevier: Amsterdam, 1984.

(25) Gung, B. W.; Wolf, M. A. *J. Org. Chem.* **1996**, *61*, 232.

(26) Tomoda, S.; Senju, T. *Chem. Lett.*, **1999**, in press.